Applied Mathematical Modelling 33 (2009) 2874–2881

Contents lists available at ScienceDirect

Applied Mathematical Modelling

journal homepage: www.elsevier.com/locate/apm

Diffusion of methylene blue in glass fibers – Application of the shrinking core model

Debasish Sarkar [a], Sampa Chakrabarti [a], Binay K. Dutta [b,*]

[a] Department of Chemical Engineering, University of Calcutta, 92, Acharya P.C. Road, Kolkata 700 009, India
[b] Department of Chemical Engineering, Universiti Teknologi PETRONAS, Malaysia

ARTICLE INFO

Article history:
Received 30 March 2008
Received in revised form 23 August 2008
Accepted 28 August 2008
Available online 6 September 2008

Keywords:
Diffusion
Shrinking core model
Sorption of methylene blue
Mathematical model

ABSTRACT

Diffusion of mass in a solid cylinder with concentration dependent diffusivity (or temperature-dependent thermal conductivity in case of heat diffusion) does not admit of an analytical solution except in special cases. The 'shrinking core model' has been used to develop an approximate analytical solution in certain circumstances. The model, generally useful to describe heterogeneous solid–fluid reactions, is applied to theoretically analyze the adsorption–diffusion phenomena of *methylene blue* dye in a glass fiber in the present work. Theoretical equations have been derived for the case of diffusivity as an exponential function of concentration. The diffusivity parameters are evaluated by global minimization of the error between the experimental and the theoretical concentration history. Other forms of diffusivity, namely constant diffusivity and diffusivity varying linearly with concentration are found to involve larger errors. A parametric sensitivity analysis of the error has been done. The shrinking core model could satisfactorily interpret the experimental dye concentration profile in the substrate.

1. Introduction

Adsorption and diffusion of small molecules such as hydrogen and water vapor in glass have received considerable attention in recent years. Adsorbed water, in particular, undergoes reversible hydrolytic reactions with the silica network in glass substantially influencing its properties. This phenomenon is especially important for optical fibers used in communication systems. The diffusion equation based on Fick's law with or without chemical reaction has been found appropriate for the theoretical analysis of transport of adsorbed molecules in the glass phase. The phenomena of mass or heat diffusion in different geometries and physical situations have been treated extensively in the literature [1–4]. If diffusion is accompanied by a chemical reaction, an analytical solution of the problem may become more difficult to arrive at. A few theoretical and numerical solutions of diffusion in the glassy phase with or without reaction have been reported. Doremus [5] analyzed experimental data on diffusion of water vapor in glass in conjunction with the solution of unsteady state reaction–diffusion equation. Mazumder [6] reported a detailed mathematical and numerical analysis of the reaction–diffusion equation in cylindrical glass phase. Similar theoretical and experimental studies on diffusion and reaction of hydrogen and water vapor have been undertaken by a few other workers as well [7–9]. Yang et al. [10] studied both theoretically and experimentally surface diffusion of propane and butane in porous Vycor glass in relation to its potential application for product separation in a membrane reactor. Diffusion of *Rhodamine* 6G, a fluorescent dye, on a glass surface in a moist environment was studied by Mitani et al. [11] and the experimental data were interpreted by a two-dimensional equation for surface diffusion of the dye.

* Corresponding author. Tel.: +60 5 368 7624; fax: +60 5 365 6176.
E-mail addresses: deba_1s@rediffmail.com (D. Sarkar), sampac@vsnl.net (S. Chakrabarti), binaydutta@petronas.com.my, binaykdutta@yahoo.com (B.K. Dutta).

0307-904X/$ - see front matter © 2008 Elsevier Inc. All rights reserved.
doi:10.1016/j.apm.2008.08.019

Nomenclature

C	liquid phase concentration at time t (mg/L), same as bulk concentration at the same time
C_0	initial liquid phase concentration (mg/L)
$C_{ij}^{*\,\mathrm{exp}}$	experimental value of dimensionless concentration of ith data point in jth run
$C_{ij}^{*\,\mathrm{model}}$	model predicted dimensionless concentration at time of Ith experimental data point in jth run
D	effective concentration dependent pore diffusivity for the proposed model (cm^2/s)
$\mathbf{D}$	concentration independent parameter vector of diffusivity–concentration relation, described in Eq. (12)
D_0	constant parameters of diffusivity in exponential, linear and constant diffusivity model (cm^2/s)
E	function of average square error
k_0	Langmuir isotherm constant (L/mg)
L	length of glass wool fiber (cm)
$N(t)$	rate of adsorption (mg/s)
n	dimensionality of an optimization problem
R	radius of a glass fiber (cm)
R_f	radius of the unused core at time t (cm)
t	time (s)
V	volume of the batch (L)
W	mass of adsorbent (g)
Y_{et}	solid phase concentration at time t (mg/g)
Y_S	Langmuir isotherm constant (L/g)
$\overline{Y}_t$	average solid phase concentration at time t (mg/g)

Greek symbols

α	exponential coefficient of concentration in effective pore diffusivity for the proposed model (L/mg)
β	linear coefficient of concentration in effective pore diffusivity for the linear model (L/mg)
ρ	adsorbent density (g/L)

Subscripts

0	initial
i	data point index
j	index of experimental run
t	at time t

Superscript

$*$	non-dimensional

In a recent paper, Chakrabarti and Dutta [12] reported adsorption and diffusion of *methylene blue*, a basic dye, from an aqueous solution in thin fibers of soft glass. Stereomicroscopic colored pictures of a single dye-stained fiber gave a clear indication of penetration of the dye into the glass. The equilibrium sorption data could be fitted well by the Langmuir isotherm. The unsteady state diffusion equation in an 'infinite' cylinder was used to theoretically analyze the diffusion phenomenon. Since the dye concentration in the solution phase was a function of time in batch sorption experiments, an analytical solution [12] for the case of constant dye diffusivity could be obtained using the Duhamel theorem. The concentration dependence of the diffusivity of the dye in glass in the real case was however obtained empirically by fitting the experimental time–concentration data in the solution of the diffusion equation. It was found that the diffusivity value was an exponential function of dye concentration.

Determination of diffusivities of penetrants in a variety of solids by fitting unsteady-state experimental uptake data with analytical solutions of the appropriate diffusion equations is a well-established practical technique e.g. [4,13]. In the present work an alternative theoretical analysis of diffusion of *methylene blue* in glass fibers has been presented by taking help of the 'shrinking core model'. This model is widely used in the theoretical analysis of gas–solid non-catalytic reactions [14]. Recently Jena et al. [15] used the model to analyze batch adsorption of a few organics from aqueous solutions in porous silica and in active carbon particles. Use of the model becomes especially convenient when the exact equations of unsteady state diffusion involve nonlinear or concentration-dependent parameters. Here we have adopted the shrinking core model to fit the experimental data on batch adsorption of the dye in glass fibers reported by Chakrabarti and Dutta [12]. The computational strategy adopted for estimation of the values of the parameters by global optimization has been described.

2. Theoretical analysis

Pseudo-steady state diffusion of the adsorbed *methylene blue* dye through a cylindrical shell in a glass fiber (Fig. 1) is assumed. Liquid side resistance to mass transfer has been neglected [12]. Theoretical analysis and computation of the

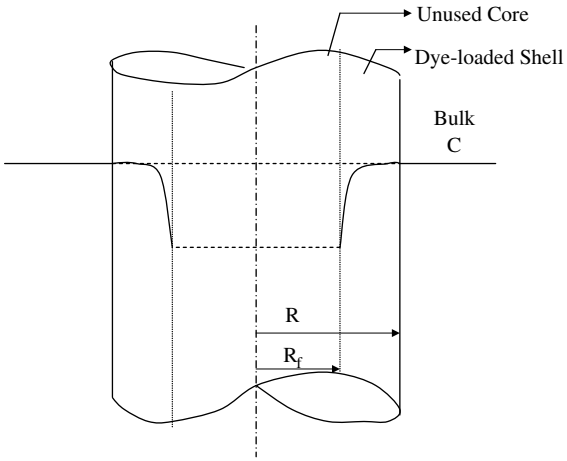

Fig. 1. Schematic diagram qualitatively showing the concentration profile of *methylene blue* in a glass fiber following the shrinking core model.

diffusivity has been done for the case in which it is an exponential function of concentration,$D = D_0\exp(-\alpha C)$. The cases of constant ($D = D_0$) as well as linearly varying diffusivity [$D = D_0(1 - \beta C)$] have also been investigated and compared.

The shrinking core model is schematically depicted in Fig. 1. If C is the dye concentration in the bulk solution at any time t, the flux of the dye in the glass fiber can be expressed as follows. The meanings of different notations used are given in the nomenclature section:

$$N(t) = \frac{2\pi L D_0[1 - \exp(-\alpha C)]}{\alpha \ln\left(\frac{R}{R_f}\right)}. \tag{1}$$

The following mass balance equation relates the shrinking rate of the virgin core and rate of change of the solid phase concentration to the instantaneous flux of the dye:

$$N(t) = \frac{\mathrm{d}}{\mathrm{d}t}[\pi L(R^2 - R_f^2)\rho Y_{et}]. \tag{2}$$

The average solid phase concentration based on the entire volume of the particle as a function of solid phase concentration in the outer shell and radius of the core [14]:

$$\overline{Y_t} = Y_{et}\left[1 - \left(\frac{R_f}{R}\right)^2\right]. \tag{3}$$

The overall mass balance equation for the entire system in terms of bulk concentration of the dye solution of volume V and average solid phase concentration:

$$-V\frac{\mathrm{d}C}{\mathrm{d}t} = W\frac{\mathrm{d}\overline{Y}_t}{\mathrm{d}t}, \tag{4}$$

where W = mass of glass fibers added to V volume of stirred solution. Now we introduce the following dimensionless variables and parameters:

$$C^* = \frac{C}{C_0}, \quad r = \frac{R_f}{R}, \quad t^* = \frac{D_0 t}{R^2}, \quad \alpha^* = \alpha C_o, \quad W^* = \frac{W}{VC_0}, \quad \rho^* = \alpha\rho.$$

In order to represent the equilibrium relation between solid and liquid phase concentration, the well-known Langmuir isotherm is used:

$$Y_{et} = \frac{Y_S C}{1 + k_0 C}. \tag{5}$$

Here k_0 and Y_S are constant parameters of the Langmuir isotherm. The dimensionless form of Eq. (5) can be written as

$$Y_{et} = \frac{Y_S^* C^*}{1 + k_0^* C^*}, \tag{6}$$

where $k_0^* = k_0 C_0$ and $Y_S^* = Y_S C_0$.

Taking the derivative of Eq. (6) w.r.t. dimensionless time t^*, we get the following relation:

$$\frac{dY_{et}}{dt^*} = \frac{Y_S^*}{(1+k_0^*C^*)^2}\cdot\frac{dC^*}{dt^*}. \tag{7}$$

Simplifying Eqs. (1) and (2) in terms of the parameters in dimensionless form

$$\frac{2[1-\exp(-\alpha^*C^*)]}{\rho^*\ln\left(\frac{1}{r}\right)} = -\frac{2rY_S^*C^*}{(1+k_0^*C^*)}\cdot\frac{dr}{dt^*} + (1-r^2)\frac{d}{dt^*}\left(\frac{C_t^*Y_S^*}{1+k_0^*C^*}\right). \tag{8}$$

Incorporating (7) in Eq. (8),

$$\frac{2[1-\exp(-\alpha^*C^*)]}{\rho^*Y_S^*\ln\left(\frac{1}{r}\right)} = -\frac{2rC^*}{(1+k_0^*C^*)}\cdot\frac{dr}{dt^*} + \frac{1-r^2}{(1+k_0^*C^*)^2}\cdot\frac{dC^*}{dt^*}. \tag{9}$$

Again simplifying Eq. (4) using Eqs. (3) and (6):

$$\frac{dr}{dt^*} = \left[\frac{\frac{1}{W^*}+\frac{(1-r^2)Y_S^*}{(1+k_0^*C^*)^2}}{\frac{2rY_S^*C_t^*}{(1+k_0^*C^*)}}\right]\frac{dC^*}{dt^*}. \tag{10}$$

Finally, solving Eqs. (9) and (10), the time evolution equation for both bulk concentration and radius of the unreacted core in their dimensionless form are as obtained:

$$\frac{dC^*}{dt^*} = -\frac{2W^*[1-\exp(-\alpha^*C^*)]}{\rho^*\ln\left(\frac{1}{r}\right)} \tag{11}$$

and

$$\frac{dr}{dt^*} = -\left[\frac{1+\frac{W^*(1-r^2)Y_S^*}{(1+k_0^*C^*)^2}}{\rho^*r\ln\left(\frac{1}{r}\right)\cdot\frac{Y_S^*C^*}{(1+k_0^*C^*)}}\right]\cdot[1-\exp(-\alpha^*C^*)]. \tag{12}$$

The initial conditions for Eqs. (11) and (12) are taken as $C^* = 1.0$ and $r = 0.999$ (rather than $r = 1$ in order to avoid singularity in the process of computation) at $t^* = 0.0$. Eqs. (11) and (12) can be solved simultaneously to find the time evolution of bulk concentration, provided all other process parameters are known. The two still unknown constant parameters in the expression for diffusivity, namely D_0 and α, can be estimated by using a suitable global optimization technique in order to achieve best fit condition of model predictions with experimental results. Computations are also carried out for the other two cases mentioned before: (a) diffusivity as a linear function of concentration [i.e., $D = D_0(1-\beta C)$] and (b) constant diffusivity [$D = D_0$]. The equations corresponding to Eqs. (11) and (12) for these cases can be derived as

$$\frac{dC_t^*}{dt^*} = -\frac{2W^*[C^* - \frac{\beta^*C^*}{2}]}{\rho_l^*\cdot\ln\left(\frac{1}{r}\right)} \tag{13}$$

and

$$\frac{dr}{dt^*} = -\left[\frac{1+\frac{W^*(1-r^2)Y_S^*}{(1+k_0^*C^*)^2}}{\rho_l^*.r\ln\left(\frac{1}{r}\right)\cdot\frac{Y_S^*C^*}{(1+k_0^*C^*)}}\right]\cdot[C^* - \frac{\beta^*C^{*2}}{2}] \quad \text{for } D = D_0(1-\beta C), \tag{14}$$

where $\rho_l^* = \frac{\rho}{C_0}$ and $\beta^* = \beta C_0$. Similarly, for the constant diffusivity case, the equivalent equations are

$$\frac{dC^*}{dt^*} = -\frac{2W^*}{\rho_l^*.\ln\left(\frac{1}{r}\right)}\cdot C^* \tag{15}$$

and

$$\frac{dr}{dt^*} = -\left[\frac{1+\frac{W^*(1-r^2)Y_S^*}{(1+k_0^*C^*)^2}}{\rho_l^*\cdot r\ln\left(\frac{1}{r}\right)\cdot\frac{Y_S^*C^*}{(1+k_0^*C^*)}}\right] \quad C_t^* \quad \text{for } D = D_0. \tag{16}$$

3. Computational methodology

Eqs. (11) and (12) are numerically solved by fourth order Runge–Kutta method using a tested step size of $\Delta t^* = 10^{-5}$ with simultaneous global optimization of the two parameters of the proposed exponential diffusivity model, D_0 and α^* described

above, so that the deviation between the computed and the experimental concentration of the dye in a glass fiber becomes minimum. The same procedure is repeated for the linear model [Eqs. (13) and (14)] as well as for the constant diffusivity model [Eqs. (15) and (16)]. The following objective function for global optimization is used:

$$E(\mathbf{D}) = \frac{1}{3} \cdot \sum_{j=1}^{3} \sum_{i=1}^{9} (C_{ij}^{*\text{model}} - C_{ij}^{*\exp})^2. \tag{17}$$

The experimental data reported by Chakrabarti and Dutta [12] on transient dye uptake by glass fibers are used for parameter estimation. Nine experimental data points ($i = 1,9$) distributed over the time span of 3 h are compared with theoretical prediction at the same instant and calculated squared error, after squaring is summed and subsequently averaged for three different experimental runs ($j = 1,3$), that began with three different initial concentrations. Since all other parameters are constant, the average square error, E, must be solely dependent on $\mathbf{D}$, where

$$\mathbf{D} = \begin{bmatrix} D_0 \\ \alpha \end{bmatrix} \quad \text{for the exponential model} \tag{18a}$$

$$= \begin{bmatrix} D_0 \\ \beta \end{bmatrix} \quad \text{for the linear model} \tag{18b}$$

$$= [D_0] \quad \text{for the constant diffusivity model.} \tag{18c}$$

The function E is minimized by the sequential simplex method [16]. The algorithm involves generation of a regular geometric pattern of $(n + 1)$ vertices where $n = 2$ is the dimensionality of the present problem. For the exponential and linear two-parameter diffusivity models, an equilateral triangle having vertices at three different initial base points 1($\mathbf{D_1}$), 2($\mathbf{D_2}$) and 3($\mathbf{D_3}$) is generated. The objective function E is evaluated at the vertices. The vertex displaying the maximum deviation is reflected through the centroid in order to generate a new vertex. The process is repeated till the error comes within the specified limit. Since the optimization problem is one-dimensional for the constant diffusivity model, it is solved by simple Fibonacci search technique [16].

4. Results and discussion

The Langmuir parameters for the given system as well as the time–concentration data for batch adsorption have been reported by Chakrabarti and Dutta [12]. In the present work dimensionless concentration–time data generated numerically after solving Eqs. (11) and (12) with simultaneous optimization of mentioned parameters (for the exponential diffusivity model) are compared with experimental values. Solutions are also generated for the other two cases of linear variation of diffusivity with concentration [Eqs. (13) and (14)] and for the constant diffusivity case [Eqs. (15) and (16)]. Fig. 2 shows a comparative plot of model prediction and experimental data at three different initial dye concentrations ($C_0 = 50$, 40 and 25 mg/L) along with the predictions of the linear and constant diffusivity models. The computed averaged squarred error of the predictions for the three different diffusivity models compared to the experimental results over all the three data sets (each consisting of nine data points) is presented in Table 1.

It is seen that the exponential model for diffusivity gives the best agreement with the experimental data among the three. The plot of the squarred error against time (Fig. 3) gives a better picture of how the error in prediction varies with the

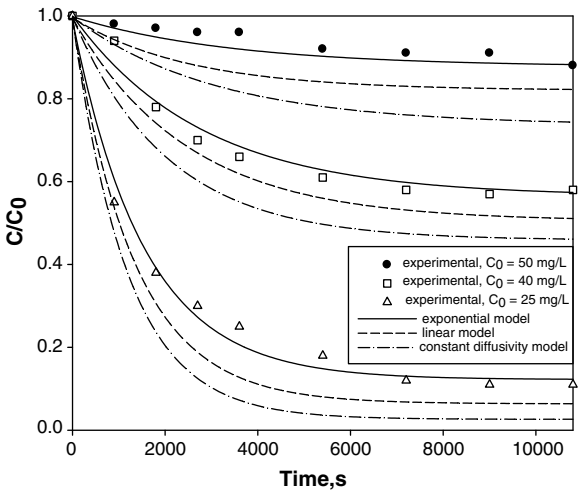

Fig. 2. Experimental [12] and predicted concentration history for various initial concentrations of the dye in solution.

Table 1
Error estimates for the three models

Diffusivity model	Error estimate $E(\mathbf{D}) = \frac{1}{3}\sum_{j=1}^{3}\sum_{i=1}^{9}(C_{ij}^{*\text{model}} - C_{ij}^{*\text{exp}})$
Exponential	5.59×10^{-3}
Linear	4.02×10^{-2}
Constant	0.12

diffusion time. For the exponential diffusivity model the squared error approaches to a value close to zero at a large time. The comparison between the experimental and predicted values are also reported in the form of a parity diagram [Fig. 4] for each of the three models. It is evident from the results that the exponential model of diffusivity works best in terms of prediction accuracy; the linear model comes next, whereas the constant diffusivity model exhibits the highest deviation from the experimental data. The shrinkage speed of unused core as predicted by the proposed model is also reported by plotting dimensionless radius (r) with respect to time as shown in Fig. 5. This plot indicates that the penetration of sorbate in the glass phase remains small even near equilibrium. This occurs due to the fact that the micro-cracks do not penetrate deep inside the glass phase.

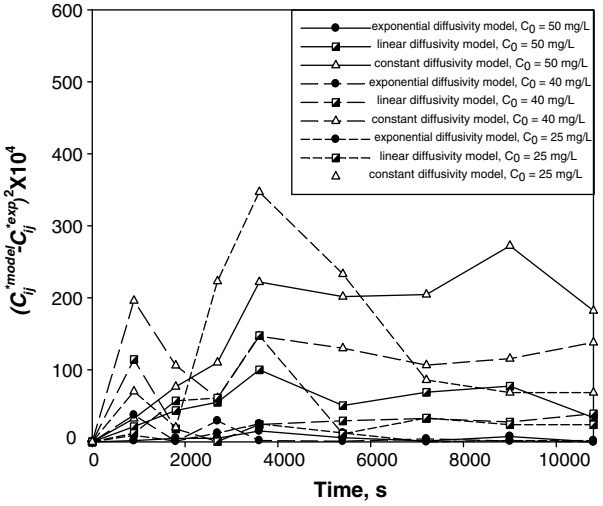

Fig. 3. Squared error for different theoretical models with respect to experimental values [12].

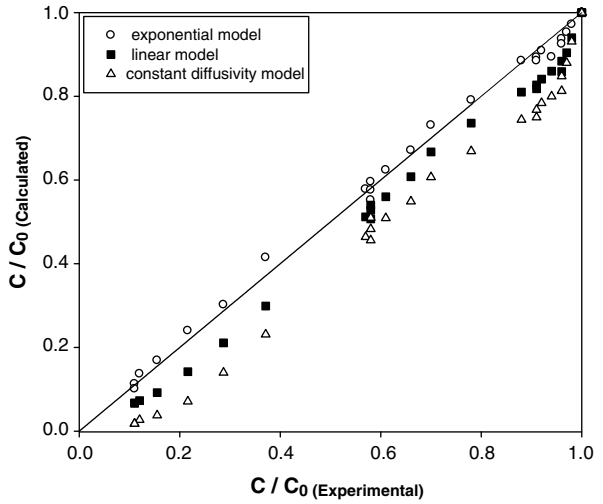

Fig. 4. Parity diagram for the experimental [12] and calculated values of C/C_0 for the three theoretical models (range of initial concentration: 25–50 mg/L).

The exponential model for the diffusivity obtained by global optimization described before can be expressed as follows:

$$D = 1.0 \times 10^{-9} \cdot \exp(-0.142C). \tag{19a}$$

The calculated pre-exponential coefficient of Eq. (19a) is the same as that of the empirical relation between diffusivity and concentration reported in our previous work [12]. However, the value of the exponential parameter, α, is a little larger. It is to be noted that D_0 and α were estimated therein by a trial-and-error procedure whereas a mathematically sound global optimization strategy has been adopted in the present work. As such, the computed value of α is more accurate. The decrease in the diffusion coefficient at a higher concentration leads to a lower penetration depth as depicted in Fig. 4 before. It has been explained in our previous paper [12] that diffusion near the surface of the glass occurs through micro-cracks. Blockage of the micro-cracks by the adsorbed molecules at a higher dye concentration appears to prevent migration of the molecules deeper into the glass phase.

It would be theoretically interesting to look into the sensitivity of error estimate on the parametric plane. An equimagnitude contour diagram of the averaged square error $E(\mathbf{D})$ is depicted as a function of the pre-exponential coefficient, D_0 and the exponential parameter, α, in Fig. 6. The figure shows that as the objective function $E(\mathbf{D})$ is multimodal and it is expectedly more sensitive towards the exponential parameter than the pre-exponential factor especially in the region close to the global

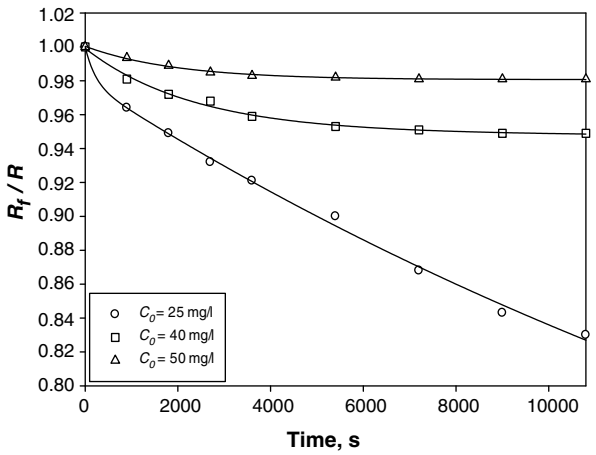

Fig. 5. Variation of dimensionless core radius with time.

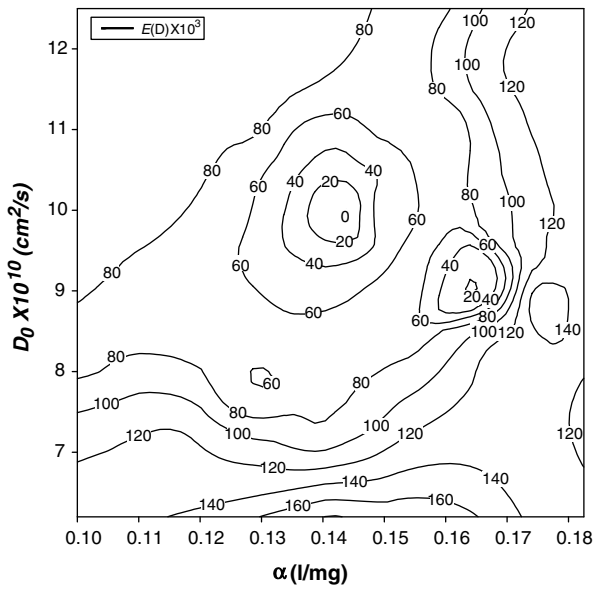

Fig. 6. Equimagnitude contour diagram of objective function, $E(\mathbf{D})$ with respect to the two adjustable parameters, D_0 and α of the proposed exponential model.

minima. For the other two models the diffusivity relations are also determined by the corresponding optimization methods and the computed diffusivity relations are given below in Eqs (19b) and (19c).

The other two computed diffusivity relations are given below in Eqs. (19b) and (19c):

$$\text{Linear model}: \quad D = 1.0 \times 10^{-9} \cdot (1 - 0.151C), \tag{19b}$$

$$\text{Constant diffusivity model}: \quad D = 9.73 \times 10^{-10}. \tag{19c}$$

5. Conclusion

The adsorption–diffusion phenomenon of *methylene blue* dye in glass fibers has been theoretically analyzed using the shrinking core model with concentration-dependent diffusivity. The model predictions were compared with the experimental data and a fair and consistent match was observed. The concentration independent parameters of diffusivity were determined by global optimization with respect to sets of experimental data at different initial concentrations. The experimental time–concentration data compared well with the predictions of exponential model for the diffusivity. The results indicate that the shrinking core model can satisfactorily describe the reaction diffusion phenomena in the glass phase.

References

[1] J. Crank, The Mathematics of Diffusion, second ed., Oxford University Press, London, 1979.
[2] M.Z.C. Lee, T.R. Marchant, Microwave thawing of cylinders, Appl. Math. Modell. 28 (2004) 711–733.
[3] K.C. Liu, P.C. Chang, Analysis of dual-phase-lag heat conduction in cylindrical system with a hybrid method, Appl. Math. Modell. 31 (2007) 369–380.
[4] F. Erdogu, Mathematical approaches for use of analytical solutions in experimental determination of heat and mass transfer parameters, J. Food Eng. 68 (2005) 233–238.
[5] R.H. Doremus, Diffusion of water in silica glass, J. Mater. Res. 95 (1995) 2379–2389.
[6] P. Mazumder, Mathematical analysis of the reaction–diffusion of water in glass tubes, J. Non-Cryst. Solids 315 (2003) 31–42.
[7] V. Lou, R. Sato, M. Tomozawa, Hydrogen diffusion in fused silica at high temperatures, J. Non-Cryst. Solids 315 (2003) 13–19.
[8] S. Berger, M. Tomozawa, Water diffusion into a silica glass optical fiber, J. Non-Cryst. Solids 324 (2003) 256–263.
[9] A. Oehler, M. Tomozawa, Water diffusion into silica glass at a low temperature under high water vapor pressure, J. Non-Cryst. Solids 347 (2004) 211–219.
[10] J. Yang, J. Cermakova, P. Uchtyl, C. Hamel, A. Seidel–Morgenstern, gas phase transport, adsorption and surface diffusion in a porous glass membrane, Catal. Today 104 (2005) 344–351.
[11] Y. Mitani, A. Shimada, S. Koshihara, K. Fukuhara, H. Kobayashi, M. Kotani, Role of adsorbed water in diffusion of rhodamine 6G on glass surface, Chem. Phys. Lett. 431 (2006) 164–168.
[12] S. Chakrabarti, B.K. Dutta, On the adsorption and diffusion of methylene blue in glass fibers, J. Colloid Interf. Sci. 286 (2005) 807–811.
[13] J.M. Vanguard, Liquid Transport Processes in Polymeric Materials, Prentice Hall, Engelwood Cliffs, NJ, 1991.
[14] J. Szekely, J.W. Evans, H.I. Sohn, Gas–Solid Reactions, Academic Press, New York, 1976.
[15] P.R. Jena, S. De, J.K. Basu, A generalized shrinking core model applied to batch adsorption, Chem. Eng. J. 95 (2003) 143–154.
[16] S.G. Beveridge, R.S. Schechter, Optimization: Theory and Practice, McGraw-Hill, Inc., 1970.